Sustainable synthesis of diamondoid ethers by high-temperature ball milling

Jasna Alić,[a,‡] Tomislav Stolar,[b,‡] Zoran Štefanić,[b] Krunoslav Užarević,[b,*] Marina Šekutor[a,*]

[a] *Division of Organic Chemistry and Biochemistry, Ruđer Bošković Institute, Bijenička 54, 10 000 Zagreb, Croatia.*

[*] E-mail: msekutor@irb.hr

[b] *Division of Physical Chemistry, Ruđer Bošković Institute, Bijenička 54, 10 000 Zagreb, Croatia.*

[*] E-mail: krunoslav.uzarevic@irb.hr

[‡] J.A. and T.S. contributed equally.

Keywords: diamondoids, thermally controlled mechanochemistry, high-temperature ball milling, sustainable organic synthesis, ethers

Abstract

Diamondoids have emerged as promising carbon-based nanomaterial building blocks because of their unique combination of exceptional properties and availability for selective functionalization. Until now, the chemical functionalization of diamondoids was primarily based on solution methods. However, the limited solubility of diamondoid derivatives and their tendency to sublimate at even slightly elevated temperatures made it difficult to prepare more extensive diamondoid derivatives. Here, we present the first mechanochemical synthesis of several diamondoid ethers differing in the type, size, and number of their hydrocarbon cage subunits. We found that the efficient preparation of these ethers is enabled solely by high-temperature ball milling conditions and does not proceed under ambient conditions. When compared to the conventional synthesis of the same ether derivatives, the calculated green chemistry metrics showed the enormous sustainability benefits of the mechanochemical synthesis. The mechanochemical approach includes shorter reaction times, a green inorganic base, a simplified workup procedure, comparable or superior reaction yields, and the elimination of solvents in the synthesis. Furthermore, crystal structures obtained from single-crystal X-ray diffraction (SCXRD) experiments confirmed the molecular structures of target products and gave insight into their intermolecular interactions in the solid state. From a perspective of the future applicability of these materials in nanotechnology, the cost and sustainability of their preparation

are paramount. We demonstrated herein that mechanochemistry is a viable option for this challenge.

Introduction

Diamondoids[1,2,3] are saturated cage hydrocarbons with a curious structural arrangement of their carbon atoms that resembles the crystal structure of a diamond.[4] Diamondoid derivatives are promising candidates for pharmaceuticals,[5] catalysis,[6,7] polymer composites,[8,9,10] host-guest systems,[11,12] light emitting devices, *etc*.[13,14,14,15,16] Furthermore, these compounds are good dispersion energy donors, which makes them valuable in studies that explore non-covalent interactions[17,18,19] and self-assembly[20,21,14] of saturated organic molecules. Because of their molecular rigidity, diverse shapes, propensity for self-association, and exceptional electronic properties when functionalized, diamondoid derivatives are applicable as nanoscale building blocks or molecular conduction junctions.[22,23,24] Additionally, monolayers of functionalized diamondoids show monochromatic electronic emission, which makes them highly promising scaffolds for the design of new nanoelectronic devices,[25,26,27] where the more extensive diamondoid derivatives (*e.g.*, [121]tetramantane-6-thiol) show more pronounced emission properties.[13,28,29] Unfortunately, the presence of higher diamondoids (from tetramantanes onwards) in crude oil is significantly lower compared to smaller analogues (adamantane, diamantane, and triamantane), making their isolation quite demanding and expensive. From a synthetic viewpoint, this lack of accessibility to larger cages can be circumvented by merging smaller and more accessible diamondoid units to build larger composites. While selective chemical functionalization of diamondoids has been systematically described in the literature,[17,30,31,32] there exist only a few examples of direct linking of two or more diamondoid cages *via* heteroatoms.[33,34,35] For instance, 1,1'-diadamantyl ether (**1**) was first reported as a side product in the synthesis of aryl adamantly ethers.[36] Afterwards, the preparation of **1** was reported by several other authors, but mainly as a by-product of various reactions.[37,38,39,40] Only recently was its first targeted synthesis reported.[13,41,42] We were intrigued by a possible preparation scope for derivatives consisting of two diamondoid cages connected by an oxygen atom. We recently reported on the synthesis and spontaneous self-assembly of ethers **1**, **2** and **4** on the highly oriented pyrolytic graphite (HOPG) surface, shedding light on the importance of London

dispersion interactions for on-surface supramolecular systems of this type.[43] However, synthesizing cage ethers that consist of two directly connected diamondoid subunits remains challenging. Diamondoid cages are quite bulky, and larger diamondoid composites often suffer from limited solubility in common organic solvents and are challenging to purify by alternative methods like sublimation. A simple and sustainable methodology for synthesizing composite diamondoid derivatives that would circumvent these reagents and product drawbacks is of great interest as it would open the way for novel nanostructured materials of this type.

In the search for more sustainable chemical synthesis, mechanochemistry imposes a viable option.[44] The use of mechanical activation drives chemical reactions forward independently on the solubility of reactants, while at the same time drastically minimizing solvent usage and waste production.[45,46,47] Mechanochemistry, therefore, provides many advantages for synthetic organic chemistry, including but not limited to overcoming solubility problems: faster reaction times, higher yields, altered selectivity, and access to products not obtainable by conventional methods.[48,49,50,51,52,53,54,55] The most used instrumental setups for mechanochemistry is vibratory ball milling, where milling jars oscillate horizontally while milling balls serve as the milling media, thus facilitating chemical transformations through mechanical activation. Furthermore, recent innovations in mechanochemistry enable conducting mechanochemical reactions at high-temperature conditions, which access reactions with high activation energies and provide control of the reaction selectivity. On the one hand, high-temperature ball milling reactions can be performed by using a heat gun that blows hot air on the milling jar.[56,57,58,59,60,61] For example, that approach was used for the synthesis of palladium-catalyzed Suzuki-Miyaura cross-coupling of insoluble aryl halides[56] and Grignard reagents in air.[57] To gain more control over the temperature of the experimental setup, we developed a modular heating element that can be attached to the milling jar and managed through a proportional-integral-derivative (PID) controller device.[62] In that way, the temperature is precisely controlled up to 250 °C and enables the use of different heating regimes. That setup was used to synthesize different derivatives containing urea and amido groups,[62] nucleophilic aromatic substitutions (S_NAr) products,[63] and prebiotic oligomerization of amino acids.[64] Moreover, high-temperature ball milling on a laboratory scale was exploited in the scale-up of the syntheses of S_NAr and Knoevenagel reactions,[65] as well as agrochemicals based on urea and gypsum cocrystals,[66] using the continuous mechanochemical manufacturing by twin-screw

extrusion. The mentioned examples demonstrate the versatility of mechanochemical synthesis and showcase a wide range of substrates. We, therefore, embarked on applying mechanochemical tools to the sustainable preparation of composite diamondoid compounds.

In this work, we report the first mechanochemical synthesis of seven tertiary diamondoid ethers, three of which are novel compounds. The prepared ethers consist of adamantanes (ethers **1** and **7**), combined adamantane and diamantane cages (ethers **2** and **4**), and solely of diamantane cages (ethers **3**, **5**, and **6**). We also performed the solution synthesis of ethers **1–6** to demonstrate the sustainability advantages of mechanochemical synthesis by green chemistry metrics. We used gas chromatography coupled with mass spectrometry (GC-MS) and nuclear magnetic resonance (NMR) spectroscopy to characterize the reaction products. The molecular structures of the target compounds were determined using single-crystal XRD experiments. Differential scanning calorimetry (DSC) was used to investigate the role of thermal energy in the synthesis of ether **1**. Mechanochemical synthesis of three-cage ether **7** demonstrated the potential of mechanochemistry in overcoming solubility problems and opened a new path to higher diamondoid derivatives.

Experimental Section

In this section, only pertinent and critical features of the experimental work are described, and more details can be found in the Supporting Information. All chemicals and solvents were purchased from commercial suppliers and used without further purification unless mentioned. Adamantan-1-ol was purchased from TCI, while diamantane alcohols were synthesized according to the literature procedure. [67] Diamondoid iodides were synthesized from corresponding alcohols and hydroiodic acid also following a literature procedure. [68] Corresponding methanesulfonates were prepared according to our recently published procedure.[43] Milling reactions were performed with InSolido Technologies vibratory ball mill using 10 mL Teflon jars placed inside a larger aluminum container. Temperature-controlled ball milling was achieved with an external 75W band heater and a PID controller according to the previously published procedure.[62] All milling reactions were conducted at 30 Hz frequency using two 7 mm stainless steel (SS) balls as a grinding media. After conducting high-temperature ball milling, the reaction was allowed to cool down to room temperature. The content of the jar was collected, and the crude reaction mixture was purified using column chromatography (SiO_2 or

Al_2O_3) to yield the corresponding diamondoid ether. ^{1}H and ^{13}C NMR spectra were recorded with Bruker AV-300 or AV-600 NMR spectrometers, and the chemical shifts were referenced to the residual proton or carbon signal of the used deuterated solvent. IR spectra were recorded with an FT-IR ABB Bomem MB 102 or FT IR-ATR PerkinElmer UATR Two spectrometers (range 400 to 4000 cm^{-1}). MALDI-TOF MS spectra were obtained in "reflectron" mode with an Applied Biosystems Voyager DE STR instrument (Foster City, CA). GC-MS analyses were performed on an Agilent 7890B/5977B GC/MSD instrument equipped with a HP-5ms column. Powder X-ray diffraction (PXRD) patterns were collected on a PanAlytical Aeris diffractometer (Cu Kα radiation and Ni filter) in Bragg-Brentano geometry using a zero background sample holder. DSC analysis was performed using Simultaneous Thermal Analyzer (STA) 6000 (PerkinElmer, Inc.) in a platinum crucible with a cap (non-hermetically sealed). Around 5 mg of each sample was analyzed using a 10 °C/min heating rate and under 20 mL/min nitrogen gas flow. Data was processed in Pyris Data Analysis software. We have used EMOS power consumption meter P5801 to measure the power consumption. Crystal structures reported herein were deposited in the CSD and were allocated the following CCDC deposition numbers: 2192585 (**3**), 2192733 (**5**), 2192586 (**6**), and 2192587 (**7**). These data contain the supplementary crystallographic information for this paper and can be obtained free of charge from the Cambridge Crystallographic Data Centre via www.ccdc.cam.ac.uk/data_request/cif.

Results and Discussion

We first milled 1-iodoadamantane (**1a**) and adamantan-1-ol (**1b**) using K_2CO_3 as a base at room temperature for 3 h. Ball milling was performed at 30 Hz in Teflon jars using two 7 mm SS balls as a milling media (more details can be found in the Supporting Information). Analysis by GC-MS showed that 1,1'-diadamantyl ether (**1**) did not form under these reaction conditions (Table 1, entry 1, Figure S1). We then used a recently devised temperature-controlled ball milling setup[62] to increase the milling reactor temperature to 100 °C while keeping the other reaction parameters constant. Encouragingly, this resulted in trace amounts of **1** (Table 1, entry 2, Figure S2). By further raising the milling temperature, conversion to **1** also increased and reached 60 % for milling at 180 °C, according to GC-MS analysis (Table 1, entries 3-5, Figures S3-S5). We also tested the use of other solid bases, such as $NaHCO_3$, K_2HPO_4, and DABCO, which exhibited lower or similar conversion rates compared to K_2CO_3 (Table 1, entries 8-10). As expected, the

control experiment performed without using a solid base did not result in conversion to **1** (Table 1, entry 14). Furthermore, we studied how the amount of the solid base affected the reactivity towards **1**. Using 1 equiv. of K_2CO_3 decreased the conversion to **1** (Table 1, entry 6), while using five equivalents resulted in the same conversion rate as in the case of 3 equivalents. (Table 1, entry 7). On the other hand, using 0.1 equiv. of K_2CO_3 did not yield **1** (Table 1, entry 15), thus showing that K_2CO_3 does not act as a catalyst.

Table 1. Optimization of the reaction conditions for the synthesis of 1,1'-diadamantyl ether (**1**) under ball milling conditions.

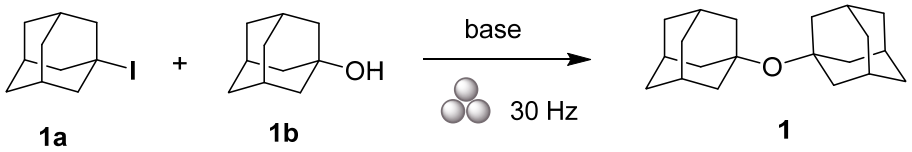

entry	time (h)	base (equiv)	temperature (°C)	GCMS yield of 1 (%)
1	3	K_2CO_3 (3)	25	0
2	3	K_2CO_3 (3)	100	1
3	3	K_2CO_3 (3)	140	24
4	3	K_2CO_3 (3)	160	40
5	3	K_2CO_3 (3)	180	60
6	3	K_2CO_3 (1)	180	54
7	3	K_2CO_3 (5)	180	60
8	3	$NaHCO_3$ (3)	180	37
9	3	K_2HPO_4 (3)	180	60
10	3	DABCO (3)	180	64
11	3	K_2CO_3 (3)	200	67 (65)*
12	1	K_2CO_3 (3)	200	47
13	6	K_2CO_3 (3)	200	71
14	3	no base	180	0
15	3	K_2CO_3 (0.1)	180	0

*isolated yield

To determine whether an even higher milling temperature would aid the conversion to **1**, we milled **1a** and **1b** with 3 equivalents of K_2CO_3 for three hours at 200 °C. Indeed, under these reaction conditions, GC-MS analysis showed that 67 % of **1** had formed (Table 1, entry 11, Figure S6), which was the highest conversion thus far. The dependence of conversion to **1** on the

milling temperature is almost linear, with a slight increase when comparing milling at 180 °C and 200 °C (Figure 1). We also investigated the effect of different reaction times, namely one hour and six hours (Table 1, entries 12 and 13). The latter revealed that three hours provides the most optimal balance between the reaction time and the conversion to **1**. Close inspection of the obtained GC-MS chromatograms revealed the presence of **1b**, while **1a** was either not present or was present only in trace amounts (Figures S5 and S6). We hypothesized that the rapid consumption of **1a** and the inability to obtain higher conversion rates might be due to the instability of **1a** at milling temperatures above 160 °C. To better understand the latter, we performed milling of **1a** with 3 equivalents of K_2CO_3 for three hours at 200 °C. This resulted in 51 % of **1** and 49 % of **1b**, most likely due to partial decomposition of **1a** into **1b** under the abovementioned conditions (Figure S7). To try to overcome this limitation, we performed milling with an excess of **1a**, which proved to be unsuccessful. We also tested the condensation reaction between 1-bromoadamantane and **1b** resulting in 44 % of **1**. Lower conversion when using 1-bromoadamantane could be due to a lower tendency of the bromide compared to the iodide to act as a leaving group. This was further validated by adding catalytic amounts of KI to the described reaction mixture, which resulted in a 60 % conversion to **1**.

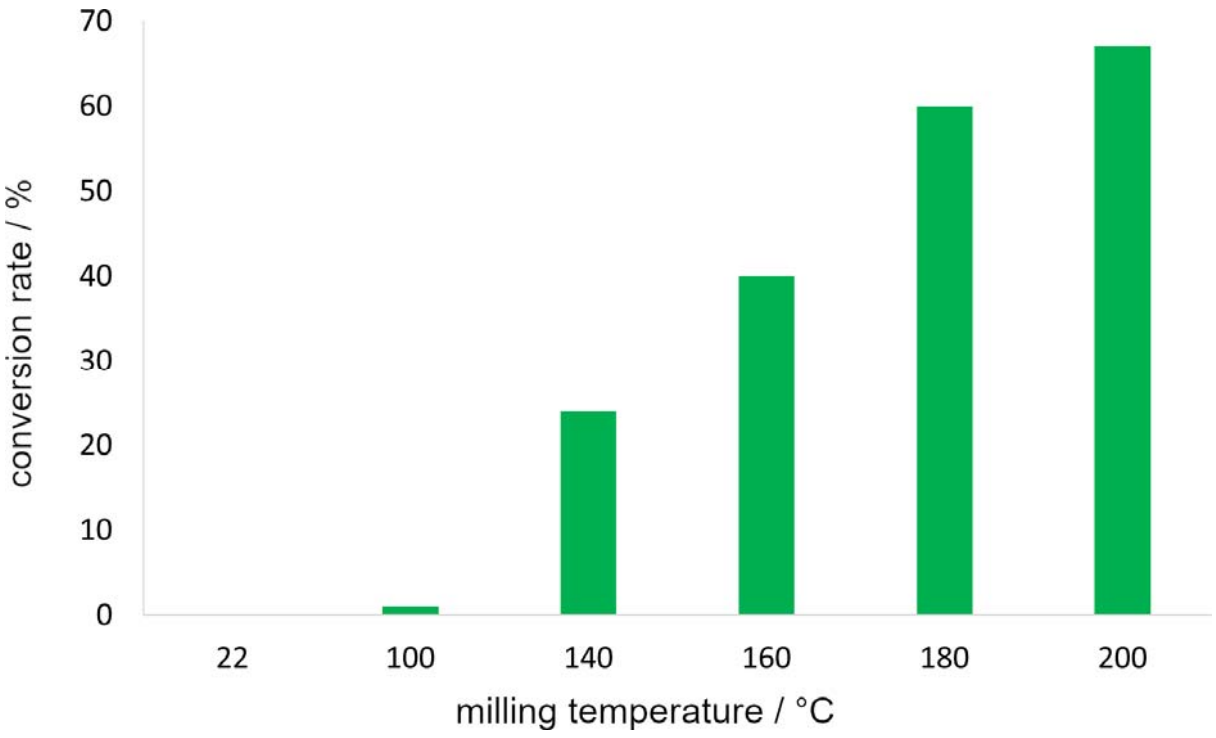

Figure 1. Influence of the milling temperature on the conversion rate to 1,1'-diadamantyl ether (**1**). Only the milling temperature was varied, and all other reaction parameters were constant.

At this point, it was clear that the milling temperature drastically affected the formation of ether **1**. Therefore, we were interested in decoupling the effects of thermal and mechanical activation on the reaction at hand. To achieve this, **1a**, **1b**, and K_2CO_3 were gently ground in a mortar and pestle. Subsequently, we performed a DSC experiment in a nitrogen atmosphere by heating the reaction mixture to 200 °C in a closed platinum pan using a 10 °C/min heating rate. As a result, the DSC trace exhibited three endotherms (Figure 2). The first endotherm at 73 °C corresponded to the melting of **1a** (Figures S8 and S9). The second one at 92 °C was attributed to the transition of the low-temperature ordered phase of **1b** to the disordered high-temperature phase with a partial amount of non-hydrogen bonded hydroxyl groups (Figures S10, S11, and S12).[69,70] Finally, the third endotherm around 134 °C corresponded to the interaction of **1a** and K_2CO_3 (Figure S13) and subsequent formation of **1** (Figure S14 and S15). As expected, DSC heating of pure **1a** did not form **1** (Figure S9).

Next, by opening the jar after ball milling at 140 °C, we observed that the reaction mixture was liquified (Figure S16). Under these conditions, a 24 % conversion to **1** was observed (Table 1, entry 3). Note that after gently mixing **1a**, **1b** and K_2CO_3 with the spatula in the milling jar (without milling it) and heating in the oven for 3 h at 200 °C, 43 % of **1** was observed (Figure S17). Furthermore, by milling **1a**, **1b** and K_2CO_3 at room temperature for 1 h and subsequent heating in the oven for 3 h at 200 °C, 49 % of **1** was observed, thus showing the positive effect of milling (Figure S18). We can therefore conclude that the formation of **1** occurs at elevated temperatures without the milling; however, in a lower conversion rate by solely thermal activation when compared to the synergistic thermal and mechanical activation provided by high-temperature ball milling.

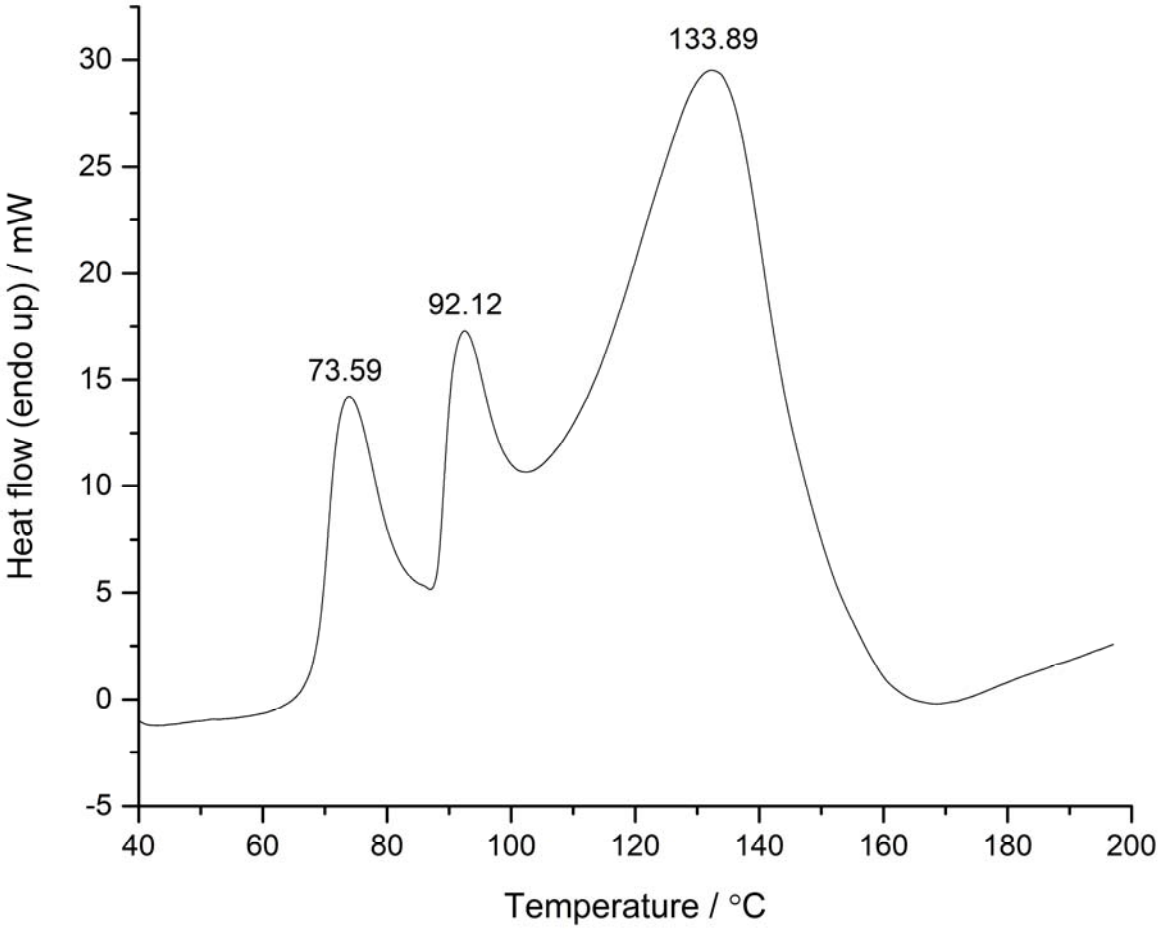

Figure 2. DSC trace of **1a**, **1b**, and K_2CO_3.

With these findings, we performed a high-temperature ball milling synthesis of ethers **2**–**6** (Figure 3). The diamantane cage, unlike the adamantane, possesses two types of tertiary carbon atoms, medial and apical, which differ in their chemical reactivity (Figure 3, denoted on compound **6**).[71,72] Our substrate scope, therefore, included mixed ethers comprised of the adamantane and the diamantane scaffold, as well as solely of diamantane cages connected in a combination of medial and apical positions.

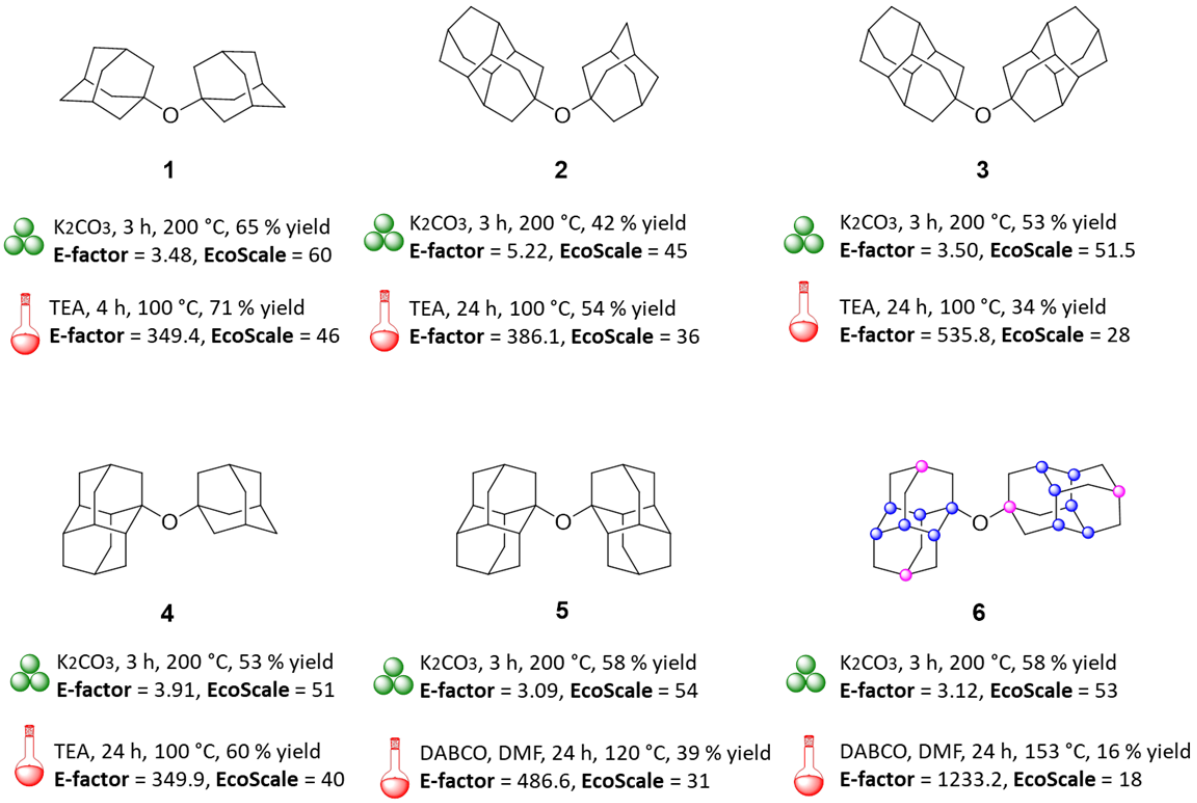

Figure 3. Comparison of the green chemistry metric for the mechanochemical and conventional preparation methods for target diamondoid ethers **1**–**6**. All metric values were calculated using the isolated yields. The medial positions of the diamantane cage are marked in blue, and the apical ones are in pink (structure **6**).

Ethers **2** and **3** were synthesized by milling 4-iododiamantane (**2a**) adamantan-1-ol (**1b**) or diamantan-4-ol (**3a**) and K_2CO_3 at 200 °C for 3 hours in 42 % and 53 % yield, respectively (Figure 3). The same reaction conditions were applied to prepare ethers **4**, **5**, and **6** (Figure 3). In these reactions, we milled 1-iododiamantane (**4a**) with the corresponding alcohol and obtained 53 %, 58 %, and 58 % yields, respectively. Note that in the preparation of ether **4**, when using 1-iodoadamantane **1a** we obtained 40 % of the product, while when 1-iododiamantane (**4a**) was a reactant, **4** was obtained with a 56 % yield. This reduction in the reaction efficiency when **1a** is used instead of **4a** may be due to a difference in the carbocation stability since the diamantane framework produces a more stable carbocation than the adamantane cage.[73,71]

To compare ball milling with conventional synthesis (neat or solution-based) of diamondoid ethers, we also performed the synthesis of ethers **1**, **2**, and **4** following our previously reported procedure,[43] as well as the synthesis of ethers **3**, **5**, and **6** that were described for the first time in this work (note that we also reported characterization of ether **3** in the mentioned previous work where we obtained it as a by-product). Some smaller diamondoid derivatives typically tend to sublimate even at slightly elevated temperatures which then prevents their interaction with other components of the reaction mixture. To avoid this problem, solution-based synthesis of diamondoid ethers was performed in an autoclave. Conventional synthesis of ethers **1**–**4** included condensing the corresponding diamondoid methanesulfonate and alcohol in the presence of TEA at 100 °C for 4-24 hours. Note that we could not successfully introduce a bulky mesylate group in the sterically more hindered medial position of the diamantane cage. The syntheses of ethers **5** and **6** were therefore performed using iodide derivatives in the presence of the DABCO base. The attempt to prepare T-shaped ether **6** from 4-diamantyl methanesulfonate (**2c**) and diamantan-1-ol (**4b**) resulted in formation of ether **3**, indicating partial hydrolysis of the mesylate derivative and its subsequent reaction with the newly formed apical alcohol. Although medial alcohol **4b** was present in excess, only trace amounts of ether **6** formed, hence pointing towards a selective attack of the less hindered hydroxyl group in the apical position of one diamantane cage on the apical carbocation present on the other diamantane cage. However, condensing **4a** with diamantan-4-ol yielded 16 % of ether **6** after heating in DMF for 24h at approximately 153°C. After performing all the described reactions, we also confirmed the molecular structures of the newly synthesized ethers **3**, **5** and **6** by solving their crystal structures from SCXRD data (Figure S19). Further details of the performed synthesis and the obtained yields of each product are given in the Supporting Information.

To showcase that ball milling is a suitable method for the preparation of even larger diamondoid ether derivatives that could serve as building blocks in materials design, we prepared a three-cage derivative consisting of three adamantane cages connected *via* two respective ether bonds (Figure 4). Ether **7** was obtained in 20% yield by milling adamantan-1,3-diol (**7a**) and 1-iodoadamantane (**1a**) with K_2CO_3 for 3h at 200°C. The molecular structure of target ether **7** was also confirmed by solving the crystal structure from the SCXRD data.

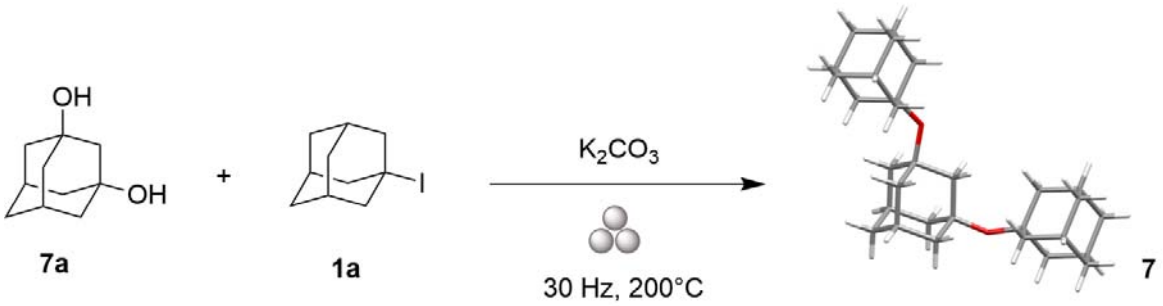

Figure 4. Reaction conditions for the synthesis of 1,3-bis(1-adamantyloxy)adamantane (**7**). The molecular structure of **7** was confirmed by solving the crystal structure from the SCXRD data.

X-ray analysis of single crystals of ethers **3**, **5**–**7** showed a tendency of dense solid-state packing with close intermolecular contacts (Figure 5). All four crystal packings are dominated by weak dispersion interactions between the cages, similar to diamondoid ethers **1**, **2** and **4** reported earlier (Figure S20).[43]

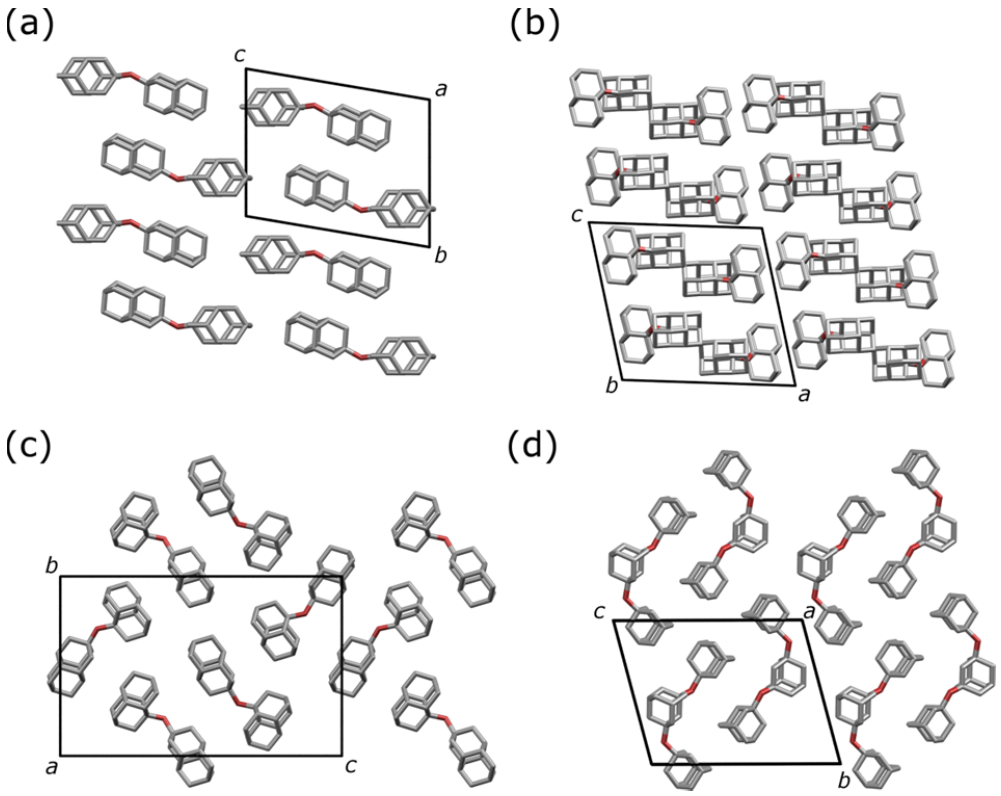

Figure 5. Packing of molecules obtained from the x-ray crystal structures of (a) **3** (triclinic $P\bar{1}$ space group), (b) **5** (monoclinic $P2_1/c$ space group), (c) **6** (orthorhombic $P2_12_12_1$ space group), (d) **7** (triclinic $P\bar{1}$ space group).

The main objective of this work was to develop a sustainable synthetic methodology for preparing tertiary diamondoid ethers which could serve as stable and rigid blocks in nanomaterial design. From the thermal input point of view, the mechanochemical synthesis of diamondoid ethers requires higher temperatures compared to conventional synthesis. In the latter, the reactants are pressurized and homogenized with TEA or solvent, and the temperature activation of 80–120 °C is sufficient for the reaction to proceed. In high-temperature ball milling, the formation of ether **1** is enabled at approximately 140 °C (Table 1, entry 3), thus demonstrating that higher activation energy is needed for the reaction to proceed under mechanochemical conditions. The rigid polycyclic structure of diamondoids prevents back-side nucleophilic attack, thus leaving the unimolecular nucleophilic substitution (S_N1) as a viable mechanism for substitution reactions. However, the detailed mechanism of the mechanochemical formation of diamondoid ethers is unknown, and further research is needed to reveal the factors for the stabilization of the carbocation intermediate in the melt.

Nevertheless, the thorough analysis of green chemistry metrics, *e.g.*, E-factor and EcoScale, highlighted the benefits of mechanochemistry when compared to the conventional synthesis (Figure 3, for details, see S6 in the Supporting Information).[74,75] Even when the conventional synthesis is performed using only TEA and without the solvent in a condensation step (ethers **1** to **4**, Figure 3), E-factor, which is defined as the ratio of the mass of total waste formed per mass of the end product, is still much greater and hence less environmentally friendly when compared to the mechanochemical procedure. Additionally, EcoScale measures the viability of the reaction not only by considering the effects of the solvent and the reaction yield but also by the price of the used chemicals, safety, and product purification procedures. In our case, higher EcoScale values again indicated that mechanochemistry is a more sustainable approach for the synthesis of diamondoid ethers when compared to conventional synthetic methods. For example, the reaction yield of ether **1** is slightly higher in the case of conventional synthesis, but EcoScale is far more favorable for the mechanochemical synthesis of **1** (60 in mechanochemical procedure, 46 in

conventional procedure), highlighting the advantage of using K_2CO_3 and avoiding the extraction step in product isolation. Also, E-factor of 3.48 in the mechanochemical approach to ether **1** shows enormous waste reduction compared to E-factor of 349.4 in its solvent-based counterpart. Moreover, the superiority of the mechanochemical method is also manifested in a significantly shortened reaction time (which is not included in the EcoScale calculation), in much simpler synthetic routes, as well as in the use of an inorganic base. Even when the yields in conventional synthesis are somewhat higher, using a mechanochemical procedure is of considerable environmental benefit. Finally, power consumption of 0.429 KWh for the high-temperature ball milling synthesis of ether **4** versus 1.821 KWh for its solution synthesis in an autoclave with magnetic stirring (reaction conditions as represented in Figure 3) highlights the energy savings of the high-temperature ball milling approach. Similarly, power consumption of 0.428 KWh for the high-temperature ball milling synthesis of ether **1** (Table 1, entry 11) versus 1.498 KWh for pre-milling and subsequent oven heating at 200 °C for 3 h demonstrates the energy consumption benefits of the high-temperature mechanochemical approach.

Conclusion

In summary, here presented study was focused on mechanochemical and conventional approaches for the synthesis of bulky diamondoid ethers **1**–**6**. The mechanochemical procedures were found to be faster, allowed for the use of the inorganic and green base, resulted in comparable or superior reaction yields, and were overall more sustainable and energy-saving. High-temperature ball milling conditions used in our work show the critical role of thermal activation in the mechanochemical synthesis of diamondoid ethers. For ether **1**, controllable heating overcomes the energetic barriers but also induces high mobility of reaction components through partial melting, increasing conversion to the final product. The decomposition of diamondoid iodides while interacting with K_2CO_3 under mechanochemical conditions is a competitive reaction to the ether formation and represents a limiting factor for achieving even higher reaction yields. The demonstrated application of mechanochemistry in the synthesis of larger three-cage diamondoid derivative **7** opens up a sustainable approach to the synthesis of next-generation materials consisting of diamondoid subunits, independently of the solubility of the reactants. More favorable green chemistry metrics of the mechanochemical approach

demonstrate that it is a viable tool for the sustainable synthesis of complex, rigid, and thermodynamically stable diamondoid materials regardless of their solubility. Furthermore, our findings showcase the possibility of performing nucleophilic substitution reactions without using solvents to stabilize the cationic intermediates, which opens a new direction for nucleophilic substitution of saturated polycyclic hydrocarbons. On-surface behavior and electronic emission properties of newly prepared ethers are currently under investigation.

ASSOCIATED CONTENT

Supporting Information. Experimental details, spectra, crystallographic data, and green metrics details can be found in the Supporting Information and are available free of charge *via* the Internet at http://pubs.acs.org.

The authors declare no competing financial interest.

AUTHOR INFORMATION

Corresponding Authors

*E-mail: krunoslav.uzarevic@irb.hr, msekutor@irb.hr

ORCID

Jasna Alić: 0000-0002-8289-5826

Tomislav Stolar: 0000-0002-9824-4462

Zoran Štefanić: 0000-0002-3486-4291

Krunoslav Užarević: 0000-0002-7513-6485

Marina Šekutor: 0000-0003-1629-3672

Author Contributions

‡ J.A. and T.S. contributed equally to the work.

ACKNOWLEDGMENT

We acknowledge financial support from the Croatian Science Foundation, HRZZ, UIP-2017-05-9653. K. U. acknowledges financial support for IP-2020-02-4702.

Synopsis

High-temperature mechanochemistry enables solvent-free synthesis of technologically important diamondoid derivatives differing in type, size, and number of their hydrocarbon cage subunits.

References

[1] Schwertfeger, H.; Fokin, A. A.; Schreiner, P. R. Diamonds are a chemist's best friend: diamondoid chemistry beyond adamantane. *Angew. Chem. Int. Ed.* **2008**, *47*, 1022−1036. DOI: 10.1002/anie.200701684

[2] Dahl, J. E.; Liu, S. G.; Carlson, R. M. K. Isolation and structure of higher diamondoids, nanometer-sized diamond molecules. *Science* **2003**, *299*, 96−99. DOI: 10.1126/science.1078239

[3] Pirali, O.; Vervloet, M.; Dahl, J. E. P.; Carlson, R. M. K.; Tielens A. G. G. M.; Oomens, J. Infrared spectroscopy of diamondoid molecules: new insights into the presence of nanodiamonds in the interstellar medium. *Astrophys. J.* **2007**, *661*, 919–925. DOI: 10.1086/516731

[4] Mcintosh, G. C.; Yoon, M.; Berber, S.; Tomanek, D. Diamond fragments as building blocks of functional nanostructures. *Phys. Rev. B.* **2004**, *70*, 045401–045408. DOI: 10.1103/PhysRevB.70.045401

[5] Wanka, L.; Iqbal, K.; Schreiner, P. R. The lipophilic bullet hits the targets: medicinal chemistry of adamantane derivatives. *Chem. Rev.* **2013**, *113*, 3516–604. DOI: 10.1021/cr100264t

[6] Nasrallah, H.; Hierso, J. Porous materials based on 3-dimensional Td-directing functionalized adamantane scaffolds and applied as recyclable catalysts. *Chem. Mater.* **2019**, *31*, 619–642. DOI: 10.1021/acs.chemmater.8b04508

[7] Agnewfrancis, K. A.; Williams, C. M. Catalysts containing the adamantane scaffold. *Adv. Synth. Catal.* **2016**, *358*, 675–700. DOI: 10.1002/adsc.201500949

[8] Yeung, K.-W.; Dong, Y.; Chen, L.; Tang, C.-Y.; Law, W.-C.; Tsui, G. C.-P. Nanotechnology of diamondoids for the fabrication of nanostructured systems. *Nanotechnol. Rev.* **2020**, *9*, 650–669. DOI: 10.1515/ntrev-2020-0051

[9] Fu, S.-Q.; Guo, J.-W.; Zhu, D.-Y.; Yang, Z.; Yang, C.-F.; Xian, J.-X.; Li, X. Novel halogen-free flame retardants based on adamantane for polycarbonate. *RSC Adv.* **2015**, *5*, 67054–67065. DOI: 10.1039/C5RA10887J

[10] Koike, K.; Araki, T.; Koike, Y. A highly transparent and thermally stable copolymer of 1-adamantyl methacrylate and styrene. *Polym. Int.* **2015**, *64*, 188–195. DOI: 10.1002/pi.4794

[11] Voskuhl, J.; Waller, M.; Bandaru, S.; Tkachenko, B. A.; Fregonese, C.; Wibbeling, B.; Schreiner, P. R.; Ravoo, B. J. Nanodiamonds in sugar rings: an experimental and theoretical investigation of cyclodextrin–nanodiamond inclusion complexes. *Org. Biomol. Chem.* **2012**, *10*, 4524–4530. DOI: 10.1039/C2OB06915F

[12] Zhang, J.; Feng, Y.; Ishiwata, H.; Miyata, Y.; Kitaura, R.; Dahl, J. E. P.; Carlson, R. M. K.; Shinohara, H.; Tománek, D. Synthesis and transformation of linear adamantane assemblies inside carbon nanotubes. *ACS Nano* **2012**, *6*, 674–8683. DOI: 10.1021/nn303461q

[13] Ochmann, L.; Kessler, M. L.; Schreiner, P. R. Alkylphosphinites as synthons for stabilized carbocations. *Org. Lett.* **2022**, *24*, 1460–1464. DOI: 10.1021/acs.orglett.2c00042

[14] Yang, W.L.; Fabbri, J. D.; Willey, T. M.; Lee, J. R. I.; Dahl, J. E. P.; Carlson, R. M. K.; Schreiner, P. R.; Fokin, A. A.; Tkachenko, B. A.; Fokina, N. A.; Meevasana, W.; Mannella, N.; Tanaka, K.; Zhou, X. J.; Buuren, T. v.; Kelly, M. A.; Hussain, Z.; Melosh, N. A.; Shen, Z.-X. Monochromatic electron photoemission from diamondoid monolayers. *Science* **2007**, *316*, 1460–1462. DOI: 10.1126/science.1141811

[15] Yan, H.; Narasimha, K. T.; Denlinger, J. D.; Li, F. H.; Mo, S. K.; Hohman, J. N.; Dahl, J. E. P.; Carlson, R. M. K.; Tkachenko, B. A.; Fokin, A. A.; Schreiner, P. R.; Hussain, Z.; Shen, Z. X.; Melosh, N. A. Monochromatic photocathodes from graphene-stabilized diamondoids. *Nano Lett.* **2018**, *18*, 1099–103. DOI: 10.1126/science.1141811

[16] Guan, H.-M.; Hu, Y.-X.; Xiao, G.-Y.; He, W.-Z.; Chi, H.-J.; Lv, Y.-L.; Li, X.; Zhang, D.-Y.; Hu, Z.-Z. Novel adamantane-bridged phenanthroimidazole molecule for highly efficient full-color organic light-emitting diodes. *Dyes Pigm.* **2020**, *177*, 108273–108280. DOI: 10.1016/j.dyepig.2020.108273

[17] Schreiner, P. R.; Chernish, L. V.; Gunchenko, P. A.; Tikhonchuk, E. Y.; Hausmann, H.; Serafin M.; Schlecht, S.; Dahl, J. E. P.; Carlson, R. M. K.; Fokin, A. A. Overcoming lability of extremely long alkane carbon–carbon bonds through dispersion forces. *Nature* **2011**, *477*, 308–311. DOI: 10.1038/nature10367

[18] Fokin, A. A.; Chernish, L. V.; Gunchenko, P. A.; Tikhonchuk, E. Y.; Hausmann, H.; Serafin, M.; Dahl, J. E. P.; Carlson, R. M. K.; Schreiner, P. R. Stable alkanes containing very long carbon-carbon bonds. *J. Am. Chem. Soc.* **2012**, *134*, 13641–13650. DOI: 10.1021/ja302258q

[19] Ebeling, D.; Šekutor, M.; Stiefermann, A.; Tschakert, J.; Dahl, J. E. P.; Carlson, R. M. K.; Schirmeisen, A.; Schreiner, P. R. London dispersion directs on-surface self-assembly of [121]tetramantane molecules. *ACS Nano* **2017**, *11*, 9459–9466. DOI: 10.1021/acsnano.7b05204

[20] Yan, H.; Hohman, J. N.; Li, F. H.; Jia, C.; Solis-Ibarra, D.; Wu, B.; Dahl, J. E. P.; Carlson, R. M. K.; Tkachenko, B. A.; Fokin, A. A.; Schreiner, P. R.; Vailionis, A.; Kim, T. R.; Devereaux, T. P.; Shen, Z.-X.; Melosh, N. A. Hybrid metal–organic chalcogenide nanowires with electrically conductive inorganic core through diamondoid-directed assembly. *Nat. Mater.* **2017**, *16*, 349–355. DOI: 10.1039/d2tc00366j

[21] King, E. M.; Gebbie, M. A.; Melosh, N. A. Impact of rigidity on molecular self-assembly. *Langmuir* **2019**, *35*, 16062–16069. DOI: 10.1021/acs.langmuir.9b01824

[22] Karlen, S. D.; Ortiz, R.; Chapman, O. L.; Garcia-Garibay, M. A. Effects of rotational symmetry order on the solid state dynamics of phenylene and diamantane rotators. *J. Am. Chem. Soc*. **2005**, *127*, 6554–6555. DOI: 10.1021/ja042512+

[23] Drummond, N. D.; Williamson, A. J.; Needs, R. J.; Galli, G. Electron emission from diamondoids: A diffusion quantum Monte Carlo study. *Phys. Rev. Lett.* **2005**, *95*, 096801–096804. DOI: 10.1103/PhysRevLett.95.096801

[24] Clay, W. A.; Dahl, J. E. P.; Carlson, R. M. K.; Melosh, N. A.; Shen, Z.-X. Physical properties of materials derived from diamondoid molecules. *Rep. Prog. Phys.* **2015**, *78*, 016501–016521. DOI: 10.1088/0034-4885/78/1/016501

[25] Clay, W. A.; Liu, Z.; Yang, W.; Fabbri, J. D.; Dahl, J. E.; Carlson, R. M. K.; Sun, Y.; Schreiner, P. R.; Fokin, A. A.; Tkachenko, B. A.; Fokina, N. A.; Pianetta, P. A.; Melosh, N.; Shen, Z. – X. Origin of the monochromatic photoemission peak in diamondoid monolayers. *Nano Lett.* **2009**, *9*, 57–61. DOI: 10.1021/nl802310k

[26] Clay, W. A.; Maldonado, J. R.; Pianetta, P.; Dahl, J. E. P.; Carlson, R. M. K.; Schreiner, P. R.; Fokin, A. A.; Tkachenko, B. A.; Melosh, N. A.; Shen, Z.-X. Photocathode device using diamondoid and cesium bromide films. *Appl. Phys. Lett.* **2012**, *101*, 241605–241609. DOI: 10.1063/1.4769043

[27] Ishiwata, H.; Acremann, Y.; Scholl, A.; Rotenberg, E.; Hellwig, O.; Dobisz, E.; Doran, A.; Tkachenko, B. A.; Fokin, A. A.; Schreiner, P. R.; Dahl, J. E. P.; Carlson, R. M. K.; Melosh, N.; Shen, Z.-X.; Ohldag, H. Diamondoid coating enables disruptive approach for chemical and magnetic imaging with 10 nm spatial resolution. *Appl. Phys. Lett*, **2012**, *101*, 163101–163105. DOI: 10.1063/1.4756893

[28] Fokin, A. A.; Schreiner, P. R. Band gap tuning in nanodiamonds: first principle computational studies. *Mol. Phys.* **2009**, *107*, 823–830. DOI: 10.1080/00268970802649625

[29] Zimmermann, T.; Richter, R.; Knecht, A.; Fokin, A. A.; Koso, T. V.; Chernish, L. V.; Gunchenko, P. A.; Schreiner, P. R.; Möller, T.; Rander, T. Exploring covalently bonded diamondoid particles with valence photoelectron spectroscopy. *J. Chem. Phys*. **2013**, *139*, 084310–084316. DOI: 10.1063/1.4818994

[30] Gunawan, M. A.; Hierso, J.-C.; Poinsot, D.; Fokin, A. A.; Fokina, N. A.; Tkachenko, B. A.; Schreiner, P. R. Diamondoids: functionalization and subsequent applications of perfectly defined molecular cage hydrocarbons. *New J. Chem.* **2014**, *38*, 28−41. DOI: 10.1039/C3NJ00535F

[31] Fokin, A. A.; Zhuk, T. S.; Pashenko, A. E.; Dral, P. O.; Gunchenko, P. A.; Dahl, J. E. P.; Carlson, R. M. K.; Koso, T. V.; Serafin, M.; Schreiner, P. R. Oxygen-doped nanodiamonds: synthesis and functionalizations. *Org. Lett.* **2009**, *11*, 3068-3071. DOI: 10.1021/ol901089h

[32] Schreiner, P. R.; Fokina, N. A.; Tkachenko, B. A.; Hausmann, H.; Serafin, M.; Dahl, J. E. P.; Liu, S.; Carlson, R. M. K.; Fokin, A. A. Functionalized nanodiamonds: triamantane and [121]tetramantane. *J. Org. Chem.* **2006**, *71*, 6709–6720. DOI: 10.1021/jo052646l

[33] Köllhofer, A.; Plenio, H. Homogeneous catalysts supported on soluble polymers: Biphasic Sonogashira coupling of aryl halides and acetylenes using MeOPEG-bound phosphine-palladium

catalysts for efficient catalyst recycling. *Chem. Eur. J.* **2003**, *9*, 1416–1425. DOI: 10.1002/chem.200390161

[34] Wagner, C. E.; Mohler, M. L.; Kang, G. S.; Miller, D. D.; Geisert, E. E.; Chang, Y.-A., Fleischer, E. B.; Shea, K. J. Synthesis of 1-boraadamantaneamine derivatives with selective astrocyte vs C6 glioma antiproliferative activity. A novel class of anti-hepatitis C agents with potential to bind CD8. *J. Med. Chem.* **2003**, *46*, 2823–2833. DOI: 10.1021/jm020326d

[35] Akhrem, I.; Orlinkov, A.; Vitt, S. Unprecedented facile reactions of propane and cycloalkanes with elemental sulfur leading to dialkylsulfides and dicycloalkylsulfides. *Inorg. Chim. Acta* **1998**, *280*, 355–359. DOI: 10.1016/S0020-1693(98)00233-3

[36] Kraatz, U. Notiz zur Synthese von 1-Adamantylaryläthern. *Chem. Ber.* **1973**, *106*, 3096–3096. DOI: 10.1002/cber.19731060941

[37] Lloris, M. E.; Marquet, J.; Moreno-Manas, M. Alxylations of α-methyl substituted β-diketones throught their Cu(II) complexes. Preparation of sterically congested β-diketones. *Tetrahedron Lett.* **1990**, *31*, 7489−7492. DOI: 10.1016/s0040-4039(00)88524-x

[38] Lloris, M. E.; Gálvez, N.; Marquet, J.; Moreno-Mañas, M. Reactions of copper(II) β-diketonates under free radical conditions. Preparation of highly congested β-diketones. *Tetrahedron* **1991**, *47*, 8031–8042. DOI: 10.1016/S0040-4020(01)81955-4

[39] Creary, X.; Willis, E. D.; Gagnon, M. Carbocation-forming reactions in ionic liquids. *J. Am. Chem. Soc.* **2005**, *127*, 18114–18120. DOI: 10.1021/ja0536623

[40] Tsypin, V. G.; Pevzner, M. S.; Golod, E. L. Oxidative alkylation of azoles: VII.* Adamantylation of azoles via oxidative generation of 1-adamantyl cations. *Russ. J. Org. Chem.* **2001**, *37*, 1762–1766. DOI: 10.1023/A:1013938527863

[41] Quesada Moreno, M. M.; Pinacho, P.; Pérez, C.; Šekutor, M.; Schreiner, P. R.; Schnell, M. London dispersion and hydrogen bonding interactions in bulky molecules: The case of diadamantyl ether complexes. *Chem. Eur. J.* **2020**, *26*, 10817–10825. DOI: 10.1002/chem.202001444

[42] Quesada Moreno, M. M.; Pinacho, P.; Pérez, C.; Šekutor, M.; Schreiner, P. R.; Schnell, M. Do docking sites persist upon fluorination? The diadamantyl ether-aromatics challenge for rotational spectroscopy and theory. *Chem. Eur. J.* **2021**, *27*, 6198–6203. DOI: 10.1002/chem.202100078

[43] Alić, J.; Biljan, I.; Štefanić, Z.; Šekutor, M. Preparation and characterization of non-aromatic ether self-assemblies on a HOPG surface. *Nanotechnology* **2022**, *33*, 355603–355614. DOI: 10.1088/1361-6528/ac6e72

[44] Ardila-Fierro, K. J.; Hernández, J. G. Sustainability assessment of mechanochemistry by using the twelve principles of green chemistry**.** *ChemSusChem* **2021**, *14*, 2145–2162. DOI: 10.1002/cssc.202100478

[45] James, S. L.; Adams, C. J.; Bolm, C.; Braga, D.; Collier, P.; Friščić, T.; Grepioni, F.; Harris, K. D. M.; Hyett, G.; Jones, W.; Krebs, A.; Mack, J.; Maini, L.; Orpen, A. G.; Parkin, I. P.; Shearouse, W. C.; Steed, J. W.; Waddell, D. C. Mechanochemistry: opportunities for new and cleaner synthesis. *Chem. Soc. Rev.* **2012**, *41*, 413–447. DOI: 10.1039/c1cs15171a

[46] Do, J.-L.; Friščić, T. Mechanochemistry: a force of synthesis. *ACS Cent. Sci.* **2017**, *3*, 13–19. DOI: 10.1021/acscentsci.6b00277

[47] Michalchuk, A. A. L.; Boldyreva, E. V.; Belenguer, A. M.; Emmerling, F.; Boldyrev, V. V. Tribochemistry, mechanical alloying, mechanochemistry: what is in a name**?** *Front. Chem.* **2021**, *9*, 685789. DOI: 10.3389/fchem.2021.685789

[48] Hernández, J. G.; Bolm, C. Altering product selectivity by mechanochemistry. *J. Org. Chem.* **2017**, *82*, 4007–4019. DOI: 10.1021/acs.joc.6b02887

[49] Andersen, J.; Mack, J. Mechanochemistry and organic synthesis: from mystical to practical. *Green Chem.* **2018**, *20*, 1435–1443. DOI: 10.1039/C7GC03797J

[50] Tan, D.; Friščić, T. Mechanochemistry for Organic Chemists: An Update. *Eur. J. Org. Chem.* **2018**, *2018*, 18–33. DOI: 10.1002/ejoc.201700961

[51] Štrukil, V. Mechanochemical organic synthesis: the art of making chemistry green. *Synlett* **2018**, *29*, 1281–1288. DOI: 10.1055/s-0036-1591868

[52] Kubota, K.; Ito, H. Mechanochemical cross-coupling reactions. *Trends Chem.* **2020**, *2*, 1066–1081. DOI: 10.1016/j.trechm.2020.09.006

[53] Bento, O.; Luttringer, F.; El Dine, T. M.; Pétry, N.; Bantreil, X.; Lamaty, F. Sustainable mechanosynthesis of biologically active molecules. *Eur. J. Org. Chem.* **2022**, e202101516. DOI: 10.1002/ejoc.202101516

[54] Howard, J. L.; Cao, Q.; Browne, D. L. Mechanochemistry as an emerging tool for molecular synthesis: what can it offer? *Chem. Sci.* **2018**, *9*, 3080–3094. DOI: 10.1039/C7SC05371A

[55] Virieux, D.; Delogu, F.; Porcheddu, A.; García, F.; Colacino, E. Mechanochemical rearrangements. *J. Org. Chem.* **2021**, *86*, 13885–13894. DOI: 10.1021/acs.joc.1c01323

[56] Seo, T.; Toyoshima, N.; Kubota, K.; Ito, H. Tackling solubility issues in organic synthesis: solid-state cross-coupling of insoluble aryl halides. *J. Am. Chem. Soc.* **2021**, *143*, 6165–6175. DOI: 10.1021/jacs.1c00906

[57] Takahashi, R.; Hu, A.; Gao, P.; Gao, Y.; Pang, Y.; Seo, T.; Jiang, J.; Maeda, S.; Takaya, H.; Kubota, K.; Ito, H. Mechanochemical synthesis of magnesium-based carbon nucleophiles in air and their use in organic synthesis. *Nat. Commun.* **2021**, *12*, 6691. DOI: 10.1038/s41467-021-26962-w

[58] Kubota, K.; Endo, T.; Uesugi, M.; Hayashi, Y.; Ito, H. Solid-state C−N cross-coupling reactions with carbazoles as nitrogen nucleophiles using mechanochemistry. *ChemSusChem* **2021**, *15*, e202102132. DOI: 10.1002/cssc.202102132

[59] Takahashi, R.; Seo, T.; Kubota, K.; Ito, H. Palladium-catalyzed solid-state polyfluoroarylation of aryl halides using mechanochemistry. *ACS Catal.* **2021**, *11*, 14803–14810. DOI: 10.1021/acscatal.1c03731

[60] Gao, Y.; Feng, C.; Seo, T.; Kubota, K.; Ito, H. Efficient access to materials-oriented aromatic alkynes *via* the mechanochemical Sonogashira coupling of solid aryl halides with large polycyclic conjugated systems. *Chem. Sci.* **2022**, *13*, 430–438. DOI: 10.1039/D1SC05257H

[61] Zhang, J.; Zhang, P.; Ma, Y.; Szostak, M. Mechanochemical synthesis of ketones via chemoselective Suzuki–Miyaura cross-coupling of acyl chlorides. *Org. Lett.* **2022**, *24*, 2338–2343. DOI: 10.1021/acs.orglett.2c00519

[62] Cindro, N.; Tireli, M.; Karadeniz, B.; Mrla, T.; Užarević, K. Investigations of thermally controlled mechanochemical milling reactions. *ACS Sustainable Chem. Eng.* **2019**, *7*, 16301–16309. DOI: 10.1021/acssuschemeng.9b03319

[63] Andersen, J. M.; Starbuck, H. F. Rate and yield enhancements in nucleophilic aromatic substitution reactions via mechanochemistry. *J. Org. Chem.* **2021**, *86*, 13983–13989. DOI: 10.1021/acs.joc.0c02996

[64] Stolar, T.; Grubešić, S.; Cindro, N.; Meštrović, E.; Užarević, K.; Hernández, J. G. Mechanochemical prebiotic peptide bond formation. *Angew. Chem. Int. Ed.* **2021**, *60*, 12727–12731. DOI: 10.1002/anie.202100806

[65] Andersen, J.; Starbuck, H.; Current, T.; Martin, S.; Mack, J. Milligram-scale, temperature-controlled ball milling to provide an informed basis for scale-up to reactive extrusion. *Green Chem.* **2021**, *23*, 8501–8509. DOI: 10.1039/D1GC02174E

[66] Brekalo, I.; Martinez, V.; Karadeniz, B.; Orešković, P.; Drapanauskaite, D.; Vriesema, H.; Stenekes, R.; Etter, M.; Dejanović, I.; Baltrusaitis, J.; Užarević, K. Scale-up of agrochemical urea-gypsum cocrystal synthesis using thermally controlled mechanochemistry. *ACS Sustainable Chem. Eng.* **2022**, *10*, 6743–6754. DOI: 10.1021/acssuschemeng.2c00914

[67] Fokina, N. A.; Tkachenko, B. A.; Merz, A.; Serafin, M.; Dahl, J. E. P.; Carlson, R. M. K.; Fokin, A. A.; Schreiner, P. R. Hydroxy derivatives of diamantane, triamantane, and [121]tetramantane: selective preparation of bis-apical derivatives. *Eur. J. Org. Chem.* **2007**, *2007*, 4738–4745. DOI: 10.1002/ejoc.200700378

[68] Fokin, A. A.; Pashenko, A. E.; Bakhonsky, V. V.; Zhuk, T. S.; Chernish, L. V.; Gunchenko, P. A.; Kushko, A. O.; Becker, J.; Wende, R. C.; Schreiner, P. R. Chiral building blocks based on 1,2-disubstituted diamantanes. *Synthesis* **2017**, *49*, 2003–2008. DOI: 10.1055/s-0036-1588694

[69] Harvey, P. D.; Gilson, D. F. R.; Butler, I. S.; Phase transitions and molecular motions in adamantane derivatives: 1-adamantanol. *Can. J. Chem.* **1987**, *65*, 1757–1760. DOI: 10.1139/v87-296

[70] Salman, S. R.; Lindon, John C.; Carpenter, T. A. Observation of solid-state phase changes in adamantanols using 13C CP-MAS NMR. *Thermochim. Acta* **1994**, *232*, 171–176. DOI: 10.1016/0040-6031(94)80056-1

[71] Fokin, A. A.; Tkachenko, B. A.; Gunchenko, P. A.; Gusev, D. V.; Schreiner, P. R. Functionalized nanodiamonds part I. An experimental assessment of diamantane and computational predictions for higher diamondoids. *Chem. Eur. J.* **2005**, *11*, 7091–7101. DOI: 10.1002/chem.200500031

[72] Gund, T. M.; Nomura, M.; Williams, Jr. V. Z.; Schleyer, P. v. R. The functionalization of diamantane (congressane). *Tetrahedron Lett.* **1970**, *11*, 4875–4878. DOI: 10.1016/S0040-4039(00)99732-6

[73] Olah, G. A.; Prakash, G. K. S.; Shih, J. G.; Krishnamurty, V. V.; Mateescu, G. D.; Liang, G.; Sipos, G.; Buss, V.; Gund, T. M.; Schleyer, P. v. R. Bridgehead adamantyl, diamantyl, and related cations and dications. *J. Am. Chem. Soc.* **1985**, *107*, 2764–2772. DOI: 10.1021/ja00295a032

[74] Sheldon, R. A. Organic synthesis; past, present and future. Chem. Ind. (London), **1992**, 903–906.

[75] Aken, K. V.; Strekowski, L.; Patiny, L. EcoScale, a semi-quantitative tool to select an organic preparation based on economical and ecological parameters. *Beilstein J. Org. Chem.* **2006,** *2*, 1–7. DOI: 10.1186/1860-5397-2-3